Title: A study of glycerol hydrogenolysis over Ru-Cu/Al_2O_3 and Ru-Cu/ZrO_2 catalysts

Author: André V.H. Soares Joyce B. Salazar Derek D. Falcone Fernanda A. Vasconcellos Robert J. Davis Fabio B. Passos

PII: S1381-1169(16)30027-9
DOI: http://dx.doi.org/doi:10.1016/j.molcata.2016.01.027
Reference: MOLCAA 9759

To appear in: *Journal of Molecular Catalysis A: Chemical*

Received date: 30-10-2015
Revised date: 12-1-2016
Accepted date: 22-1-2016

Please cite this article as: André V.H.Soares, Joyce B.Salazar, Derek D.Falcone, Fernanda A.Vasconcellos, Robert J.Davis, Fabio B.Passos, A study of glycerol hydrogenolysis over Ru-Cu/Al2O3 and Ru-Cu/ZrO2 catalysts, Journal of Molecular Catalysis A: Chemical http://dx.doi.org/10.1016/j.molcata.2016.01.027

A study of glycerol hydrogenolysis over Ru-Cu/Al_2O_3 and Ru-Cu/ZrO_2 catalysts

André V. H. Soares[a,b], Joyce B. Salazar[a], Derek D. Falcone[c], Fernanda A. Vasconcellos [a]

Robert J. Davis[c] and Fabio B. Passos [a,*]

[a]*Departamento de Engenharia Química e de Petróleo, Universidade Federal Fluminense, Rua Passo da Pátria, 156, Niterói, RJ CEP 24210-240, Brazil*

[b]*Instituto Federal do Rio de Janeiro – IFRJ, Avenida República do Paraguai, 120, Sarapuí - Duque de Caxias CEP: 25050-100, Brazil*

[c]*Department of Chemical Engineering, University of Virginia, 102 Engineers Way, Charlottesville, VA 22904-4741, USA*

* Corresponding author email addresses: fbpassos@vm.uff.br (F. B. Passos)

Graphical abstract

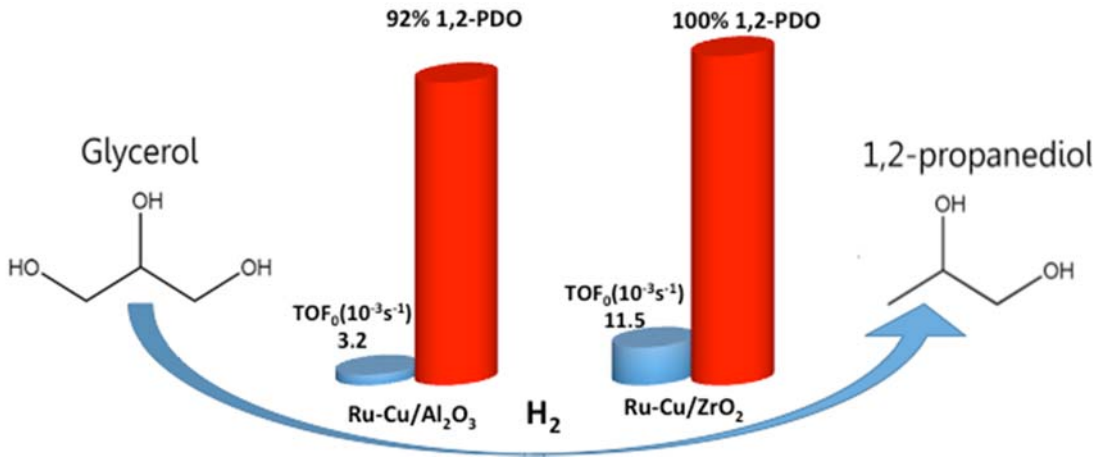

Highlights

- Ru-Cu/Al_2O_3 and Ru-Cu/ZrO_2 have been investigated in glycerol hydrogenolysis.
- Ru-Cu/ZrO_2 displayed higher turnover frequencies.
- Ru-Cu/ZrO_2 was more selective for 1,2 propanediol.
- Optimum Ru/Cu ratio was obtained.

Abstract

This work focuses on the activity, selectivity, and characterization of alumina and zirconia supported Ru(2.5%wt.)-Cu(2.5%wt.) bimetallic catalysts to produce 1,2-propanediol (1,2-PDO) from glycerol hydrogenolysis. Characterization techniques included XRD, BET, TEM, H_2 chemisorption, TPR and DRIFTS. Turnover frequencies were obtained for batch reactions ran at different temperatures. At 473 K and 2.5 MPa of dihydrogen, a conversion of 45% of glycerol with 94% selectivity towards 1,2-PDO was found when the Ru(2.5%wt.)-Cu(2.5%wt.)/Al_2O_3 was used. Recycle experiments were done for the monometallic catalysts, in which Ru/Al_2O_3 showed a better performance.

Keywords: Ruthenium; Copper; Glycerol hydrogenolysis; Propylene glycol;

1. Introduction

The search for alternative energy sources has arisen because of concerns related to the environmental impact of using fossil resources. Although the discovery of new oil and natural gas sources can postpone the complete depletion of fossil resources, the problems associated with a shortage are expected to occur within the next few decades. In this context, the quest for sustainability has become an important point in the motivation of academic and industrial

scientists and government officials in the planning and development of using renewable biomass as alternative fuels to mitigate the problem. Much of the chemical industry uses oil as the main feedstock in the production of fine chemicals, polymers, and fuels. Nowadays, there is considerable interest to generate power from biomass as well as convert it into chemicals and value-added materials [1].

Biodiesel is a high quality fuel produced by the transesterification of triglycerides, derived from renewable sources like plant oils and animal fats. This biofuel is a liquid with similar combustion properties to diesel oil but it is essentially sulfur free, which makes it more environmentally friendly [2]. Mixing 2 to 30 % biodiesel into fossil derived diesel does not require changes to engines, and will produce lower amounts of particulate matter [3]. Biodiesel has been produced on an industrial scale in Europe since 1992 encouraged by institutions and a growing public concern for the environment. In 2012, biodiesel production in Europe reached 8.6 million tons, which is slightly lower compared to previous years [4]. In Brazil, federal legislation [5] has driven a compulsory biodiesel demand, by enforcing a minimum 5% biodiesel content in all diesel fuel consumed in the country. This has led to an increase in the number of authorized production units and actual biodiesel production. As of February 2014, the total regulated monthly production of biodiesel in Brazil was 243,670 m^3, which represents only 37 % of the total authorized capacity in the country. In light of this, production growth is still expected. The Brazilian biodiesel production comes mainly from soybean oil (70.9%) and bovine fat (24.8%) [6].

For every 9 kg of biodiesel produced, about 1 kg of glycerol is formed as a byproduct. Although there are many applications for glycerol, its production has exceeded the demand, which leads to a depreciation in the value of the product [7].

In this context, the search for economic and environmentally useful alternatives for glycerol becomes imperative, in order to ensure the continuity and viability of biodiesel

production [8]. Among the promising techniques that have been developed for glycerol usage are: hydrogenolysis to produce 1,2- or 1,3-propanediol; aqueous and gas phase reforming to form CO and H_2; etherification reaction to form polyglycerols; and selective oxidation to produce ketones, acids and aldehydes [9-11].

Glycerol conversion by catalytic hydrogenation or hydrogenolysis to glycols, i.e. 1,2-propanediol (1,2-PDO), 1,3-propanediol (1,3-PDO), and ethylene glycol (EG), is an attractive process both economically and environmentally. 1,2-PDO is used for polyester resins, pharmaceuticals, antifreeze, cosmetics, and tobacco humectants. 1,3-PDO is a highly valued chemical that is mainly used in specialty polyester fibers, films, and coatings [12-13]. The various products that may be obtained from glycerol hydrogenolysis and other related reactions are shown in Figure 1.

Different catalysts have been used towards 1,2-PDO production from glycerol with and without the use of external hydrogen, and a special attention has been given to Pt catalysts promoted by other metals [14,15] and Pd catalysts [16,17]. Different groups have studied Ru catalysts yielding different conversions and selectivities towards 1,2-PDO [18-49]. In one of the earliest works on glycerol hydrogenolysis over ruthenium catalysts, Montassier et al. [19] observed that monometallic Ru catalyst preferentially breaks the C-C bond instead of the C-O bond, which results in degradation products. These authors utilized Ru/SiO_2 catalysts and found that methane was the main product, along with ethane and propane, as expected products of complete hydrogenation.

Special attention should be given to acidic promoters for Ru/C, such as Amberlyst 15, that reach a conversion of about 79% with a selectivity of 75% to 1,2-PD at 393 K, a relatively mild temperature [18]. Feng et al. [20] used a 5% Ru/Al_2O_3 to catalyze glycerol hydrogenolysis at 453 K and a hydrogen pressure of 5 MPa to obtain a conversion of 34.3 % with a 47.3 % selectivity to 1,2-PDO. As it will be shown, these reported values are similar to

those found with the home made catalysts used in this work. Lee and Moon [21] have also used 5% Ru/Al_2O_3, and obtained a 45.6 % conversion with a selectivity of 59.2 % for 1,2-PDO.

When investigating the activity of Cu catalysts, Montassier et al. [19] observed that for the Cu-Raney catalyst, under a hydrogen pressure of 3 MPa and a temperature of 513 K, 86% of the product selectivity was 1,2-PDO. Other authors have also tested copper for this reaction and obtained good selectivity for 1,2-PDO. [22-25]

The use of Ru alloys with other noble metals has been also investigated. Maris & Davis have investigated glycerol hydrogenolysis over Pt and Ru catalysts [26], as well as the effect of bimetallic Pt-Ru and Au-Ru catalysts [27], and saw levels of conversions near 100% in alkali reaction environments, with varying selectivities. The authors have seen that nonetheless Pt is less active than Ru to activate C-C bonds. Roy et al. [28] used commercial Pt/Al_2O_3 and Ru/Al_2O_3 and showed that hydrogenolysis occurred in the absence of H_2, by generating hydrogen via heterolytic cleavage of H_2O on Pt sites.

When studying the effect of Cu in Ru catalysts, Jiang et al. [29] have worked with Ru-Cu clay supported catalysts for glycerol hydrogenolysis and have seen that a decrease in Ru/Cu ratio causes a drop in conversion with a relative increase in 1,2-PDO selectivity. Rouco et al. [30] used Ru-Cu and Ru-Ag catalysts supported on silica for the hydrogenolysis of ethane and both catalysts displayed a decrease in activity when compared to the monometallic ruthenium, since Cu and Ag have a lower activity in breaking C-C bonds. Guo et al. [31] utilized Cu/Al_2O_3 under mild conditions (493 K and H_2 pressure of 1.5 MPa), yielding a 49.6 % conversion with a selectivity of 96.8 % for 1,2-PDO. Vasiliadou and co-authors [32] performed the glycerol hydrogenolysis reaction under 513 K and 8 MPa, finding a conversion of 40.5 % with a 60.5 % selectivity using Ru/ZrO_2, and a conversion of 26.7 % with a 39.7 % selectivity when using Ru/Al_2O_3.

In a work with similar interests as this one, Liu et al. [33] investigated the influence of the support on Ru-Cu catalysts. The catalysts used by those authors had a Ru/Cu atomic ratio of about 10/1 and were supported on TiO_2, SiO_2, ZrO_2, Al_2O_3, HY and NaY. They noted that Ru-Cu/ZrO_2 had the best performance. Since they observed no 1,3-PDO while acetol was present in the products, the authors have proposed a mechanism that differs from the one envisaged by Montassier et al.: dehydration of glycerol occurs first, generating acetol, then hydrogenation takes place. The difference between the two reaction pathways, (Figure 2a) from Montassier et al. [19] and (Figure 2b) from Liu et al. [33], can be seen in Figure 2. Balaraju et al. [34] have summarized the question stating that solvent medium and catalyst acidity have a great influence on reaction mechanism, thus pathway (a) is due to alkali catalysts while acetol in pathway (b) is due to acidic catalysts.

Shimizu et al. [35] have investigated the interaction of hydrogen with bimetallic Ru-Cu surfaces and have inferred that, given the non-homogeneous alloy, three different kinds of regions for Cu can be identified on the surface of the system, wherein even small percentages of Cu on the surface (>4%) may cause H_2 adsorption to drop drastically, compared to Ru adsorption. These authors have also considered that the immiscibility of the metals, and thus lack of an ensemble effect, allows the presence of various possible new adsorption sites for H_2, e.g. kink and terrace sites. Sinfelt et al. [36] studied the Ru-Cu system and found the same trend on the hydrogen chemisorption capacity that the authors above cited.

However, in our previous work [37], we investigated the interaction of bimetallic Ru-Cu/TiO_2 surfaces by XPS and the binding energies of both Ru and Cu in the bimetallic catalysts were similar compared to the monometallic catalysts and revealed no clear trend with composition, suggesting that electron transfer between the two metals in the bimetallic catalysts was minimal. We had also observed that when Cu was mixed with Ru in the given

proportion, there was a slight decrease in H/Ru, likely the result of Cu deposition onto the Ru surface of 1:1 to 1:5 Ru/Cu. In agreement to the fact that hydrogen chemisorption is not enhanced by increasing the Cu weight loading, Rouco et al. [30] found that as the nominal Cu/Ru molar ratio of a Cu-Ru/SiO_2 catalyst was increased from 0 to 0.667, the H/Ru ratio determined by H_2 chemisorption remained approximately constant.

More recently, Cu-based glycerol hydrogenolysis studies have been especially focused on the use of Y-zeolite supported catalysts [38], on the effect of preparation methods in the catalyst activity of Cu/SiO_2 [39], on Cu-Cr bimetallic sites with high Cu^0/Cu^+ ratios [40], and glycerol hydrogenolysis over Pt in tandem with methanol aqueous phase reforming (APR) over Cu:Zn:Al bulk catalysts [41]. On the other hand, Ru/TiO_2 [42,43], and Ru/zeolite systems [44,45] have been trending as proposed heterogeneous catalysts towards glycerol hydrogenolysis.

The present work has the objectives of describing the preparation, characterization, and evaluation of the performance of supported Ru-Cu bimetallic catalysts, which favor the production of 1,2-propanediol, 1,3-propanediol and ethylene glycol from glycerol hydrogenolysis. Moreover, turnover frequencies (TOF) are calculated for the Ru-Cu systems, which are scarce in the literature. Bimetallic catalysts are known to produce distinct selectivities in some reactions, especially hydrogenolysis [36]. The following characterization techniques were employed: temperature programmed reduction (TPR), X-ray diffraction (XRD), textural analysis by N_2 adsorption, H_2 chemisorption, transmission electronic microscopy (TEM), and Diffuse Reflectance Infrared Fourier Transform Spectroscopy (DRIFTS). To evaluate the influence of reaction parameters, such as hydrogen pressure, temperature, and initial concentration of glycerol, catalytic tests were performed in a high-pressure reactor.

2. Experimental

2.1. Catalyst preparation

The catalysts prepared for this work were monometallic Ru, monometallic Cu, and Ru-Cu, each supported on Al_2O_3 or ZrO_2. The loading of each metal was 2.5 wt %. The catalysts were prepared by successive incipient wetness impregnations of Ru and Cu. The catalysts were prepared using $Ru(NO)(NO_3)_3.H_2O$ (Aldrich), and $Cu(NO_3)_2.3H_2O$ (Sigma Aldrich) as the precursor salts. Al_2O_3 was obtained by calcination of boehmite (Catapal) in air for 3 h at 823 K with heating rate of 5 $K.min^{-1}$. After metal impregnation, the supported catalysts were dried at 393 K for 12h followed by calcination in air at 623 K for 4h with heating rate of 2.5 $K.min^{-1}$.

2.2. Catalyst characterization

Surface areas and pore volumes were determined by N_2 physisorption at 77 K, using the BET analysis method employing an ASAP 2010 Micromeritics analyzer. Prior to the measurements, the samples were degassed at 523 K for 6 h.

The X-Ray Diffraction (XRD) patterns were performed in a Rigaku (Miniflex II) diffractometer with a CuKα (1.540 Å) radiation.

The temperature programmed reduction (TPR) experiments were carried out on a sample (0.5 g) that was dried under flow of He (30 $mL.min^{-1}$) for 30 min at 423 K and then cooled to room temperature. Temperature programmed reduction was performed under 30 $mL.min^{-1}$ flow of a gas mixture of 5% H_2/Ar, while the samples were heated to 723 K at 10 $K.min^{-1}$. The measurements were carried out in a multipurpose unit coupled to a quadrupole mass spectrometer (Pfeiffer Vacuum, Prisma TM).

Hydrogen chemisorption was performed in a Micromeritics ASAP 2020 automated adsorption analyzer. The samples were reduced at 573 K under flowing H_2 for 60 min, and then outgassed under vacuum at 573 K for 60 min. After this, the catalysts were cooled to 308 K and evacuated again for 60 min followed by analysis at 308 K. The total amount of H_2 adsorbed was calculated by extrapolating the hydrogen uptake to zero pressure, assuming a stoichiometry H/Ru_{surf} equal to unity.

CO chemisorption measurements were carried out in the same multipurpose unit used for TPR. The catalyst samples (ca. 50 mg) were pretreated under a flow of He (30 $mL.min^{-1}$) for 30 min at 423 K and then cooled to room temperature. The activation step took place at 573 K under a flow of 5%H_2/Ar (30 $mL.min^{-1}$) for 1 h, followed by flushing under a flow of He for 30 min at 573 K and cooling to 300 K. CO uptake was measured by injecting a number of CO pulses and the exposed Ru was calculated assuming a CO/Ru molar ratio of 1/1.

Diffuse Reflectance Infrared Fourier Transform Spectroscopy (DRIFTS) of adsorbed carbon monoxide was performed with a Bruker VERTEX 70 spectrometer with a high-temperature DRIFTS cell (Harrick, HVC-DRP-4), fitted with ZnSe windows, and a diffuse reflectance accessory with Praying Mantis geometry. Spectra were acquired at a resolution of 4 cm^{-1}, typically averaging 256 scans. The samples were initially pretreated with a He flow (30 $mL.min^{-1}$) for 30 min at 423 K. Then, the temperature was raised to 573 K in pure H_2 flow (30 $mL.min^{-1}$) for 1h. After the reduction, the sample was flushed in He flow for 30 min, followed by cooling at 303 K. CO adsorption was then performed under CO/He flow (30 $mL.min^{-1}$) for 30 min at 303 K, followed by flushing of the sample for 15 min with He and before recording spectra. To determine the thermal desorption of the adsorbents, the sample temperature was increased stepwise in continuous He flow. Images of the catalysts were obtained by transmission electron microscopy (TEM) (FEI Titan) at 300 kV and a Gatan 794 Multi-scan Camera to analyze metal particle size. At least 300 particles were analyzed from

each sample. The samples were prepared by suspending the catalysts in ethanol, and agitating them in an ultrasonic bath for 10 min; then drops of the suspension were applied to a Cu mesh grid.

2.3. Catalytic tests

Glycerol hydrogenolysis reactions were carried out in a 300 mL stainless steel batch reactor (Parr 4848). The reaction conditions were: temperature of 453 K, initial hydrogen pressure of 2.5 MPa, mass of catalyst of 1.2 g and 100 mL of glycerol (20 wt% in water). The reaction time was 24 hours with stirring of 500 rpm.

Prior to the reaction, the catalyst was reduced at 573 K for 1h, in a separate unit, under a flow of pure H_2 (30 mL.min^{-1}), followed by oxidation under a flow of 5% O_2/He (15 mL min^{-1}) for 15 min at 273 K.

The reaction sequence was as follows: load the reactor with the glycerol solution and the appropriate amount of catalyst, purge with a flow of N_2 (30 mL.min^{-1}) for 5 min, and treat in flowing H_2 (30 mL.min^{-1}) at ambient temperature for 1 h in the reaction vessel. The temperature and H_2 pressure were then increased to the desired values under constant stirring. The batch reaction proceeded for a 24 h period. After 24 h, the system was cooled to ambient temperature and liquid and gaseous samples were collected. The liquid phase products were analyzed and identified by a GC-MS (Shimadzu, GCMS-QP2010S) equipped with a 95% polyethylene glycol (PEG) wax RTX column. The gas phase was sampled and analyzed in a 490 Micro-GC (Agilent) equipped with three columns: M5A 9 (H_2, O_2, N_2, CH_4 and CO), 5CB (PoraPLOT U CO_2 and C_2H_6) and PPU(CP-Sil 5CB – Hydrocarbons). CH_4 was obtained as a gas product in an amount less than 1%.

The identified products were: 1,2-PDO, 1,3-PDO and 1-propanol as products of the hydrogenolysis reaction and ethylene glycol (EG), ethanol, methanol and methane as

degradation products of glycerol. Product and reactant concentrations were calculated using measured response factors.

3. Results and discussion

3.1. Catalyst characterization

The surface areas and pore volumes of the supports and prepared catalysts are shown in Table 1. As it can be seen, for Al_2O_3 supported catalysts, there was an 8 % decrease in area by the addition of either 2.5 wt % Ru or 2.5 % Ru and 2.5 % Cu. On the other hand, for ZrO_2 supported catalysts, there was the same decrease in area when adding Ru metal, but adding both Ru and Cu had a stronger effect on the support surface area.

Figure 3 shows the X-ray diffractograms, in which five characteristic peaks for Ru and RuO_x are observed. The broadest peaks are assigned to Ru^0. There are no detected Cu peaks in the bimetallic catalyst. The Scherrer formula provides an inverse proportionality relationship between crystal size and XRD peak width, in a way that broader peaks are related to smaller particles [46]. If this relation holds for monometallic Ru/Al_2O_3 and bimetallic $Ru\text{-}Cu/Al_2O_3$, the average particle sizes lie in the range of 3.5-5 nm. Particle size analysis by TEM showed a slightly larger particle size, but they were on the same order of magnitude. On the other hand, peaks corresponding to RuO_x were not detected on the ZrO_2 supported catalyst probably because peaks from the crystalline zirconia support mask any contributions from RuO_x.

The TPR profiles for the catalysts used in this work are displayed in Figure 4, and the results of the analyses are shown in Table 2. The reduction efficiency was calculated as the amount of H_2 consumed over the theoretical amount required to reduce RuO_3 and CuO.

According to the literature, precursor salts seem to have a great effect on reduction efficiency. Many values for RuO_2 reduction temperature can be found, especially for catalysts prepared with $RuCl_3$ as a precursor salt [47-52]. Koopman et al. [47] have reported that for Ru/SiO_2, reduction of RuO_2 takes place between 450 K and 478 K, and McNicol and Short [48] have reported that there is a single peak at 443 K for bulk unsupported RuO_2. According to Hurst et al. [49], the reduction of $RuNO(NO_3)_x$ may present different profiles, depending

on the reduction of NO and the x number of NO_3 groups. Mazzieri et al. [50] reported that ruthenium oxide reduction takes place at 470 K, while a shoulder may also be seen, representing the reduction of the oxichloride for $RuCl_3$. Using $Ru(acac)_3$ as the precursor, Bianchi [51] has reported that reduction of RuO_3 to RuO_2 occurs with a small peak at 393 K, and that RuO_2 to Ru^0 takes place at 483 K with a much larger peak. In this work, monometallic Ru/Al_2O_3 showed a small peak of reduction at about 438 K, a shoulder at about 473 K, and a broader and larger peak at 558 K. From these peaks it could be inferred that the first peak represents higher oxidation states, the shoulder would be RuO_3 and the last peak RuO_2. This agrees partially with the range of reduction (450-525 K) reported by Lee and Moon [21]. The TPR profiles for monometallic Ru/ZrO_2 and Ru/Al_2O_3 obtained in this work differ notably from each other, which might be caused by different interactions of the precursor salt and the supports. The Ru/ZrO_2 catalyst shows only one broad peak that begins at 421 K and ends at about 450 K, whereas Ru/Al_2O_3 has a very broad reduction peak around 558 K.

When investigating TPR profiles for $Ru\text{-}Cu/Al_2O_3$, Galvagno et al. [52] noted that using $RuCl_3$ as the precursor salt, the addition of Cu generated a shoulder, which shifted the Ru reduction peak closer to the lower Cu reduction temperature. This was attributed to the interactions between support and the metallic salts. This is corroborated by the present work, in which it has been seen that the Cu addition favored reduction of Ru at lower temperature for $Ru\text{-}Cu/Al_2O_3$. The bimetallic $Ru\text{-}Cu/ZrO_2$ profile displayed a broader range for reduction, which is related to the addition of Cu. Since cluster formation is expected for Ru and Cu mixtures, instead of homogeneous alloys [46,53], it can be inferred that the shifts in reduction temperature may be caused by inter-phase hydrogen adsorption, which favors Cu reduction.

Another evidence of this is the observed simultaneous reduction of Cu and Ru species for the bimetallic Ru-Cu/Al_2O_3 and Ru-Cu/ZrO_2, indicating some interaction between the two metals.

Carbon monoxide DRIFTS results are shown in Figure 5. Cu/Al_2O_3 displayed a sharp peak at 2100 cm^{-1}, Ru/Al_2O_3 showed a very weak peak at 2064 cm^{-1}, and the bimetallic Ru-Cu/Al_2O_3 showed both distinct 2100 cm^{-1} and a broad peak at 2009 cm^{-1}. Gottschalk et al. [45] reported the same value of 2064 cm^{-1} for Ru/Al_2O_3. Brown and Gonzalez [55] have assigned the 2080 cm^{-1} frequency to a Ru–CO σ-bond, as the main peak for Ru/SiO_2 supported catalysts, while Unland [56] found that Ru has weak peaks at 2009 cm^{-1} and 2070 cm^{-1}, and Kim et al. [57] have associated the CO chemisorption on Cu/SiO_2 at 2125 cm^{-1}. Therefore, it can be said that while Ru had a poor performance in CO adsorption, Cu, on the other hand, acted as promoter of adsorption in the Ru-Cu/Al_2O_3 bimetallic catalyst, with a blue-shift of about 25 cm^{-1}. For the ZrO_2 supported catalysts, although Ru/ZrO_2 displayed a strong peak at 2070 cm^{-1}, in accordance with Unland [56], Cu addition blue-shifted the peak to about 2060 cm^{-1}, decreasing its amplitude. The Cu^+-CO species is known to occur at 2158 cm^{-1} for zeolites [58], and the obtained value of 2100 cm^{-1} for the intense absorbance band of Cu/Al_2O_3 could be attributed to Cu^+. The formation of Cu^{2+} sites seems to be disfavored.

TEM micrographs of the catalysts and their respective size distributions are presented in Figure 6. As it can be seen, ruthenium particles were larger for Ru/ZrO_2 than for Ru/Al_2O_3. Additionally the dimensions of bimetallic Ru-Cu/Al_2O_3 particles were somewhat more frequently larger, in the range of 8-10 nm.

The different techniques used to assess the metal particle size must be confronted with one another to capture a clear description of the dimensions of the active metallic particles. First, it should be noted that the particle size distribution derived from TEM analysis is dependent on sampling, and a truly Gaussian distribution was not obtained for Ru/ZrO_2, since

it can be clearly seen that particles with 22 nm of diameter are relevant, albeit their relative smaller amount. These large particles have a great impact in decreasing H_2 uptake given the lower amount of surface Ru, and they were not observed for Ru/Al_2O_3, which is consistent with the better dispersion measured from the H_2 chemisorption analysis. Another possible explanation is the presence of partially reduced ZrO_2, which would decorate some of the palladium particles and suppress hydrogen adsorption capacity.

3.2. Hydrogenolysis of glycerol

Glycerol conversion and the selectivity of Ru based catalysts used for the hydrogenolysis reaction are presented in Table 3. Selectivity was calculated as the ratio of product moles produced over the total moles of glycerol converted. The different sets of catalysts showed various performances towards the hydrogenolysis reaction. For all of the evaluated catalysts, the products identified were: 1,2-PDO, EG, 1,3-PDO, 1-propanol, ethanol and methanol. Methane, CO and CO_2 were also found in the gas phase, but the CO quantities were very low in comparison to all other C1 compounds.

Acetol was detected as a final product in these reactions at very low concentrations. However, Vasiliadou et al. [32] found a significant amount of acetol after 5 h of reaction. Their experiment was performed under severe conditions, using 8MPa of hydrogen pressure, at 513K and pure glycerol. The presence of acetol in every experiment was interpreted by those authors as a possible intermediate product of the dehydration/hydrogenation mechanism, which finally yields 1,2-PDO after a hydrogenation step, in agreement with the

literature [59-62]. The absence of acetol in the present work may be possibly explained by the longer duration of the reaction (24 h).

The turnover frequency was calculated using the dispersion from hydrogen chemisorption as a measure for the surface Ru active atoms, and since H_2 uptake was lower for Ru/ZrO_2, the number of active Ru atoms is also lower. The reaction rate was similar for Ru/ZrO_2 and Ru/Al_2O_3 (7.05_x10^{-7} mol/g_{cat}.s and 7.92 $_x10^{-7}$ mol/g_{cat}.s, respectively), and therefore the turnover frequency must be greater for larger particles, with comparatively fewer atoms on the surface than well dispersed catalysts.

The main identified product in all catalytic reactions studied was 1,2-PDO, except for Ru/Al_2O_3, which presented about equal quantities of 1,2-PDO and EG. The best conversion was obtained with monometallic Ru/Al_2O_3 catalyst, with a varying selectivity to possible products. When compared with Ru/ZrO_2, it could be inferred that the extra activity of alumina is due to acidity, since glycerol protonation may favor OH cleavage. The 1,3-PDO selectivity was not pronounced in practically any of the tested catalysts. The $Ru\text{-}Cu/ZrO_2$ catalyst presented the highest selectivity towards 1,2-PDO (100%) followed by $Ru\text{-}Cu/Al_2O_3$ (≈92%). Under 503 K and 8 MPa, a previous study showed that a $3\%Ru\text{-}1\%Cu/Al_2O_3$ catalyst converted 100% of glycerol with a selectivity of 85% for 1,2-PDO [29]. Table 4 shows a comparison between the tested catalysts in this work and those described in the literature. By comparing the results, although better conversion values have been reported, the selectivity obtained by this work, 91.9 %, had not been yet reported for that reaction temperature (473 K).

As it can be seen from the activity results in Table 3, the addition of Cu to Ru is responsible for an increment in the selectivity towards the production of 1,2-PDO, mainly by suppressing C-C cleavage and avoiding the formation of EG and C1 compounds. This effect does not seem to stem from the ability to chemisorb hydrogen, since our results show no clear

general trend between Cu increment and H uptake. For Ru/Al_2O_3, the addition of Cu does not affect the H uptake as considerably as in the case of ZrO_2-supported catalysts, which is low for monometallic Ru/ZrO_2, but almost triples in the case of bimetallic $Ru\text{-}Cu/ZrO_2$. Since the reduction of bimetallic particles is also overall better for the bimetallic catalysts than for monometallic Ru, as seen from our TPR results, it can be said that Cu stabilizes reduced metallic particles capable of interacting rather with terminal hydroxyl groups of glycerol than with the C-C bond.

The effect of temperature on catalyst selectivity for $Ru\text{-}Cu/Al_2O_3$ was also investigated. Although a more complex model for glycerol hydrogenolysis may be suitable, available kinetic data for glycerol conversion agree with a first order reaction. Table 5 shows the apparent specific velocity constants, k_{app}, the initial rate of consumption of glycerol per volume, $R_{V,0}$, the initial rate of consumption per catalyst gram, $R_{m,0}$, the initial turnover frequency, TOF_0, for each of the given temperatures. The squared sample correlation coefficients, r^2, for all temperatures were between 0.992 and 0.996. Although considerable difficulties are encountered in calculating the actual TOF [63], in this work the TOF was normalized by H_2 chemisorption. Upon comparing the specific velocities, and using least squares methodology, the apparent barrier energy can be shown to be 63.5 kJ/mol, which agrees with the value reported by Lahr and Shanks (62 kJ/mol) for glycerol hydrogenolysis over ruthenium [64]. It should be noted that the turnover frequencies for Ru/ZrO_2 catalysts are remarkably greater than for the other catalysts, due to the smaller number of H_2 adsorption sites that offer relatively the same apparent specific reaction velocity. The conversion range and kinetic fitting used in this article is in agreement with a prior work done by

our group with Ru-Cu/TiO_2 catalysts, cited as ref. [37], regarding TOF calculations, based on first order kinetics.

All catalysts tested in the hydrogenolysis reaction behaved as described in the corresponding literature. In the present work, Ru-Cu/ZrO_2 displayed the best 1,2-PDO yield, with 100% selectivity at low conversion, as it can be seen in table 3, with slightly less conversion compared to monometallic ruthenium, corroborating Liu et al. [33]. In the present work, monometallic Cu/Al_2O_3 catalyst did not show activity for the glycerol hydrogenolysis reaction, as seen in reference [31]. The discrepancy from the conversion obtained in this work with other referenced values [29,33] is attributed to the larger glycerol to catalyst mass ratio.

The mass ratio of glycerol/catalyst used in the present work (16.7 $g_{Glycerol}/g_{cat}$) is much larger than the ones reported by Jiang et al. (about 5.4 $g_{Glycerol}/g_{cat}$) [29], and by Liu et al. (about 6.0 $g_{Glycerol}/g_{cat}$) [33]. According to ref. [29] an optimal atomic ratio of Ru/Cu is 3:1, whereas for ref. [33] optimal ratio was found at 10:1. Since the conditions used in the present work differ greatly from the conditions used in refs. [29] and [33], regarding glycerol/catalyst mass ratios, it does not seem adequate to offer accurate comparisons. It is, however, safe to say that Ru-Cu exhibits interesting catalytic behavior in a range from 10:1 to 10:16 of Ru/Cu atomic ratios for both ZrO_2 and Al_2O_3 as supports, from which the best activities are found in the lower Cu content region, since hydrogen chemisorption is not favored by Cu in the active sites. Besides this, somewhat contradictory to refs. [29] and [33], the greater Ru/Cu fraction used in this work does not seem to have any negative effect towards 1,2-PDO production, since 100% selectivity was obtained for Ru-Cu/ZrO_2, as seen in table 3, which could point to other influencing factors in the reaction, such as solvent action.

The low specific rate per gram of catalyst tested for the reaction can be related to the low dispersion of the ruthenium particles, as showed in Table 1. The incipient wetness

impregnation method used for the preparation of the catalysts did not produce a high particle dispersion. Balaraju et al. [13] evaluated the influence of preparation methods and the metal content in TiO_2 supported ruthenium catalysts, and observed that when the catalyst was prepared by the incipient wetness impregnation the glycerol conversion (31 %) was lower than when the method was precipitation (44 %). These authors implied that the low conversion presented by the catalysts prepared by the conventional method is related to the low metal particle dispersion over the supporting material.

Recycling experiments were performed for the monometallic catalysts, the results of which can be seen in Table 6. Both Ru/Al_2O_3 and Ru/ZrO_2 catalysts showed a drop on the order of ~ 5% in activity, in the first recycle. The Ru/ZrO_2 catalyst showed the more dramatic drop in activity after the second recycle (about 58% from the first recycle). Comparatively, Al_2O_3 appears to offer a more stable support for the catalyst, exhibiting a 20 % drop from the first recycle.

By interpretation of the obtained characterization and glycerol hydrogenolysis activity data for the materials, it is possible to propose a model for the bimetallic catalysts' surfaces, as follows. The first step is to consider that Ru and Cu are highly immiscible, and given its atomic size and mass, Cu atoms are more likely to form particles on top of the Ru structure. The second step is to consider that both metals present different space group structures. While reduced Ru forms hexagonal close packed (hcp) crystals ($P6_3/mmc$), Cu forms face-centered cubic (fcc) crystals (Fm-3m). For fcc crystals, the basal plane (110) is the one with least atomic density, while the (111) plane presents the closest packing, from which hexagonal surfaces should be expected as the most stable cleavage configuration. Therefore, it is reasonable to suspect that the Cu atoms would organize themselves in hexagonal layers over already assembled bulk hcp Ru nano-particles. The third step is to consider the actual

diffractogram of Ru-Cu/Al_2O_3, in which Cu-related peaks are absent, but Ru-related peaks are prominent. The influence of Cu coverage over Ru in hydrogenolysis activity is also a function of the reduction activation temperature prior to the reaction [65]. All reactions of this work were undertaken using a reduction temperature of 573 K, around the expected temperature range indicative of Cu mobility for multilayer deposition onto Ru, but far bellow temperatures of intensive sintering (>780 K). With this in mind, since Ru-Cu homogeneous alloy formation is unlikely [63,65], given the immiscibility of both metals, multi-layer deposition of Cu occurs, but not to the extent as to cover entirely the Ru surface at the reduction temperature of 573 K, or to separate entirely Cu clusters from the Ru particles.

This is evidence for considering Ru as the bulk particle phase, with thin layers of Cu on top of it. The bimetallic structure would thus be prone to anisotropy, with parts of the Ru crystal available for coordination or chemisorption-like phenomena, while the Cu sites would also display enhanced activity, from Cu^+ sites. The monometallic Ru catalyst particles have an average diameter of 6 nm, and the bimetallic Ru-Cu catalyst particles have an average diameter of about 11 nm, from which the increased length would be due to the outer Cu cluster layers.

Finally, the effect these geometric factors have on the electron band structure for the bimetallic particle should also be considered. Both Ru and Cu are late transition metals, which is enough to envisage that electronic interactions between metallic particles and molecules will happen through sp and d bands and molecular orbitals of the adsorbate. While Cu has a completely filled, narrow d band, very near the Fermi level, Ru atoms have open shell 4d electrons, and therefore a broader d band in respect to the density of states. Thus, formation of small Cu clusters on the surface of Ru structures would create an asymmetric d band distribution along the bimetallic particle. As seen from the obtained activity data, Cu has the ability to direct selectivity towards the formation of 1,2-PDO in glycerol hydrogenolysis,

avoiding further C-C bond breaking. This points to the fact that the band distribution is such that it enables back donation to C-O molecular orbitals upon adsorption, after which the C-C orbitals can not be further filled by the modified Ru d band, but rather a hydrogenation of the adsorbed C atom takes place.

4. Conclusion

The use of ruthenium-copper bimetallic catalysts in glycerol hydrogenolysis presents a viable alternative for 1,2-PDO production. There is considerable agreement between the literature and the results obtained in the present work, which shows the highest selectivity for 1,2-PDO by usage of Ru-Cu/ZrO_2 catalyst. The turnover frequency for the Ru-Cu/ZrO_2 is greater than for the Al_2O_3 bimetallic catalyst. An optimum proportion of Ru/Cu is situated in the region of low Cu content for best relation conversion/selectivity towards 1,2-PDO, and it appears that a convenient atomic ratio is 10:1. However selective Ru-Cu/ZrO_2 is, it should be noted that Al_2O_3 is a much more stable support for glycerol hydrogenolysis.

5. Acknowledgements

J. B. Salazar, A.V.H. Soares and F. B. Passos acknowledge the financial support from CNPq, CAPES and FAPERJ. D.D. Falcone and R.J. Davis acknowledge support by the US National Science Foundation under award number CBET-1157829.

6. References

[1] L. Prati, P. Spontoni, A. Gaiassi, From Renewable to Fine Chemicals Through Selective Oxidation: The Case of Glycerol, Top Catal. 52 (2009) 288–296.

[2] C.A.G. Quispe, C.J.R. Coronaro, J.A. Carvalho Jr., Glycerol: Production, consumption, prices, characterization and new trends in combustion, Renew. Sust. Energ. Rev. 27 (2013) 475–493.

[3] A. Williams, R.L McCormick, R.R. Hayes, J. Ireland, H.L. Fang, Effect of Biodiesel Blends on Diesel Particulate Filter Performance, Powertrain and Fluid Systems Conference and Exhibition, Society of Automotive Engineers, 2006. Available at: http://savebiodiesel.com/40015.pdf, accessed on 29 June 2015.

[4] European Biodiesel Board, available at http://www.ebb-eu.org/stats.php, accessed on 29 June 2015.

[5] BRAZIL, Federal Law No. 11097, from January 13th, 2005. Available at http://www.planalto.gov.br/ccivil_03/_ato2004-2006/2005/Lei/L11097.htm, accessed on 29 June 2015.

[6] BRAZIL, Agência Nacional de Petróleo, Gás Natural e Biocombustíveis (ANP). Boletim Mensal do Biodiesel – February 2014. Available at www.anp.gov.br, accessed on 29 June 2015.

[7] G. Knothe, J. Van Gerpen, J. Krahl, L.P. Ramos, The Biodiesel Handbook, Edgar Blücher, São Paulo, 2006.

[8] C.J.A. Mota, C.X.A. Silva, V.L.C. Gonçalves, Glycerochemistry: New Products from Glycerin of Biodiesel Production, Quím. Nova 32 (2009) 639-648.

[9] K. Lehnert, P. Claus, Influence of Pt particle size and support type on the aqueous-phase reforming of glycerol, Catal. Commun. 9 (2008) 2543–2546.

[10] A. Brandner, K. Lehnert, A. Bienholz, M. Lucas, P. Claus, Production of Biomass-Derived Chemicals and Energy: Chemocatalytic Conversions of Glycerol, Top. Catal. 52 (2009) 278–287.

[11] E. Farnetti, J. Kaspar, C. Crotti, A novel glycerol valorization route: chemoselective dehydrogenation catalyzed by iridium derivatives, Green Chem. 11(2009)704–709.

[12] J.N. Beltramini, C. Zhou, Catalytic Conversion of Glycerol to Valuable Commodity Chemicals, in: Mark Crocker (Ed.) Thermochemical conversion of biomass to liquid fuels and chemicals, RSC Publishing, Cambridge, 2010, pp. 435-467.

[13] M. Balaraju, V. Rekha, B.L.A. Prabhavathi Devi, R.B.N. Prasad, P.S. Sai Prasad, N. Lingaiah, Surface and structural properties of titania-supported Ru catalysts for hydrogenolysis of glycerol, Appl. Catal. A - Gen. 384 (2010) 107–114.

[14] A.V.-H. Soares, G. Perez, F.B. Passos, Alumina supported bimetallic Pt–Fe catalysts applied to glycerol hydrogenolysis and aqueous phase reforming, Applied Catalysis B: Environmental, 185 (2016) 77-87.

[15] A. Ciftci, S. Eren, D.A.J.M. Ligthart, E.J.M. Hensen, Platinum-Rhenium Synergy on Reducible Oxide Supports in Aqueous-Phase Glycerol Reforming, Chemcatchem, 6 (2014) 1260-1269.

[16] F. Mauriello, A. Vinci, C. Espro, B. Gumina, M.G. Musolino, R. Pietropaolo, Hydrogenolysis vs. aqueous phase reforming (APR) of glycerol promoted by a heterogeneous Pd/Fe catalyst, Catalysis Science & Technology, (2015).

[17] J. Ge, Z. Zeng, F. Liao, W. Zheng, X. Hong, S.C.E. Tsang, Palladium on iron oxide nanoparticles: the morphological effect of the support in glycerol hydrogenolysis, Green Chemistry, 15 (2013) 2064-2069.

[18] Y. Nakagawa Y, K. Tomishige, Heterogeneous catalysis of the glycerol hydrogenolysis, Catal. Sci. Technol. 1 (2011) 179–190.

[19] C. Montassier, J.C. Ménézo, L.C. Hoang, C. Renaud, J. Barbier, Aqueous Polyol Conversions on Ruthenium and on Sulfur-modified Ruthenium, J. Mol. Catal. 70 (1991) 99-110.

[20] J. Feng, H. Fu, J. Wang, R. Li, H. Chen, X. Li, Hydrogenolysis of glycerol to glycols over ruthenium catalysts: Effect of support and catalyst reduction temperature, Catal. Commun. 9 (2008) 1458–1464.

[21] S.H. Lee, D.J. Moon, Studies on the conversion of glycerol to 1,2-propanediol over Ru-based catalyst under mild conditions, Catal. Today 174 (2011) 10–16.

[22] S. Wang, H. Liu, Selective hydrogenolysis of glycerol to propylene glycol on Cu-ZnO catalysts, Catal. Lett. 117 (2007) 62-67.

[23] M. Balaraju, V. Rekha, P.S. Sai Prasad, R.B.N. Prasad, N. Lingaiah, Selective Hydrogenolysis of Glycerol to 1, 2 Propanediol Over Cu-ZnO Catalysts, Catal. Lett. 126 (2008)119–124.

[24] A. Bienholtz, F. Schwab, P. Claus, Hydrogenolysis of glycerol over a highly active CuO/ZnO catalyst prepared by an oxalate gel method: influence of solvent and reaction temperature on catalyst deactivation, Green Chem. 12 (2010) 290–295.

[25] A. Bienholtz, H. Hoffmann, P. Claus, Selective hydrogenolysis of glycerol over copper catalysts both in liquid and vapour phase: Correlation between the copper surface area and the catalyst's activity, Appl. Catal. A – Gen. 391 (2011) 153–157.

[26] E.P. Maris, R.J. Davis, Hydrogenolysis of glycerol over carbon-supported Ru and Pt catalysts, J. Catal. 249 (2007) 328–337.

[27] E.P. Maris, W.C. Ketchie, M. Murayama, R.J. Davis, Glycerol hydrogenolysis on carbon-supported PtRu and AuRu bimetallic catalysts, J. Catal. 251 (2007) 281–294.

[28] D. Roy, B. Subramaniam, R.V. Chaudhari, Aqueous phase hydrogenolysis of glycerol to 1,2-propanediol without external hydrogen addition, Catal. Today 156 (2010) 31–37.

[29] T. Jiang, Y. Zhou, S. Liang, H. Liu, B. Han, Hydrogenolysis of glycerol catalyzed by Ru-Cu bimetallic catalysts supported on clay with the aid of ionic liquids, Green Chem. 11 (2009) 1000–1006.

[30] A.J. Rouco, G.L. Haller, J.A. Oliver, C. Kemball, A comparative Investigation of Silica-supported Ru-Cu and Ru-Ag catalysts, J. Catal. 84 (1983) 297-307.

[31] L. Guo, J. Zhou, J. Mao, X. Guo, S. Zhang, Supported Cu catalysts for the selective hydrogenolysis of glycerol to propanediols, Appl. Catal. A – Gen. 367 (2009) 93–98.

[32] E.S. Vasiliadou, E. Heracleous, I.A. Vasalos, A.A. Lemonidou, Ru-based catalysts for glycerol hydrogenolysis—Effect of support and metal precursor, Appl. Catal. B – Environ. 92 (2009) 90–99.

[33] H. Liu, S. Liang, T. Jiang, B. Han, Y. Zhou, Hydrogenolysis of Glycerol to 1,2-Propanediol over Ru-Cu Bimetals Supported on Different Supports, Clean–Soil Air Water 40 (2012) 318–324.

[34] M. Balaraju, K. Jagadeeswaraiah, P.S. Sai Prasad, N. Lingaiah, Catalytic hydrogenolysis of biodiesel derived glycerol to 1,2-propanediol over Cu-MgO catalysts, Catal. Sci. Technol. 2 (2012) 1967–1976.

[35] H. Shimizu, K. Christmann, G. Ertl, Model Studies on Bimetallic Cu-Ru Catalysts. 2. Adsorption of Hydrogen, J. Catal. 61 (1980) 412-429.

[36] J.H. Sinfelt, Structure of Bimetallic Clusters, Accounts Chem. Res. 10 (1977) 15-20.

[37] J.B. Salazar, D.K. Falcone, H.N. Pham, A.K. Datye, F.B. Passos, R.J. Davis, Selective production of 1,2-propanediol by hydrogenolysis of glycerol over bimetallic Ru–Cu nanoparticles supported on TiO_2, Appl. Catal. A – Gen. 482 (2014) 137-144.

[38] L. Niu, R. Wei, F. Jiang, M. Zhou, C. Liu, G. Xiao, Selective hydrogenolysis of glycerol to 1,2-propanediol on the modified ultrastable Y-type zeolite dispersed copper catalyst, React. Kinet. Mech. Cat. 113 (2014) 543-556.

[39] Z. Huang, H. Liu, F. Cui, J. Zuo, J. Chen, C. Xia Effects of the precipitation agents and rare earth additives on the structure and catalytic performance in glycerol hydrogenolysis of Cu/SiO2 catalysts prepared by precipitation-gel method, Catal. Today, 234 (2014) 223–232.

[40] Z. Xiao, X. Wang, J. Xiu, Y. Wang, C.T. Williams, C. Liang Synergetic effect between Cu^0 and Cu^+ in the Cu-Cr catalysts for hydrogenolysis of glycerol, Catal. Today, 234 (2014) 200–207.

[41] E.S. Vasiliadou, V.L. Yfanti, A.A. Lemonidou, One-pot tandem processing of glycerol stream to 1,2-propanediol with methanol reforming as hydrogen donor reaction, Appl. Catal. B - Environ. 163 (2015) 258–266.

[42] J. Feng, B. Xu, D.R. Liu, W. Xiong, J.B. Wang, Hydrogenolysis of Glycerol on Supported Ru-Co Bimetallic Catalysts, Adv. Mat. Res. 12 (2013) 791-793

[43] V.P. Kumar, Y. Harikrishna, N. Nagaraju, K.V.R. Chary, Characterization and reactivity of TiO2 supported nano ruthenium catalysts for vapour phase hydrogenolysis of glycerol, Indian J. Chem. Sect. A -Inorg. Bio-inorg. Phys. Theor. Anal., 53 (2014) 516-523.

[44] Y. Li, L. Ma, H. Liu, D. He, Influence of HZSM5 on the activity of Ru catalysts and product selectivity during the hydrogenolysis of glycerol, Appl. Catal. A - Gen. 469 (2014) 45-51.

[45] S. Jin, Z. Xiao, C. Li, C.T. Williams, C. Liang, Hydrogenolysis of glycerol over HY zeolite supported Ru catalysts, J. Energy Chem. 23 (2014) 185-192.

[46] I. Chorkendorf, J.W. Niemantsverdriet Concepts of Modern Catalysis and Kinetics. Second, Revised and Enlarged Edition, Wiley-VHC Verlag GmbH & Co. KGaA, Weinheim, 2011.

[47] P.G.J. Koopmann, A.P.G. Kieboom, H. van Bekkum, Characterization of ruthenium catalysts as studied by temperature programmed reduction, J. Catal. 69 (1981) 172-179.

[48] B.D. McNicol, R.T. Short, Short Communication: The Reducibility of Ru, Pt-Ru and Pt Oxide Electrocatalysts as Measured by Temperature-Programmed Reduction and Cyclic Voltammetry, J. Electroanal. Chem. 92 (1978) 115.

[49] N.W. Hurst, S.J. Gentry, A. Jones, B.D. McNicol, Temperature Programmed Reduction, Catal. Rev. 24 (1982) 233-309.

[50] V. Mazzieri, F. Coloma-Pascual, A. Arcoya, P.C. L'Argentière, N.S. Fígoli, XPS, FTIR and TPR characterization of Ru/Al_2O_3 catalysts, Appl. Surf. Sci. 210 (2003) 222–230.

[51] C.L. Bianchi, TPR and XPS investigations of Co/Al2O3 catalysts promoted with Ru, Ir and Pt, Catal. Lett. 76 (2001)155-159.

[52] S. Galvagno, C. Crisafulli, R. Maggiore, A. Giannetto, J. Sehwank, TPR Investigation of Bimetallic Ru-Cu samples supported on SiO_2, Al_2O_3 and MgO, J. Therm. Anal. 32 (1987) 471-483.

[53] A. Christensen, A.V. Ruban, P. Stoltze, P.W. Jacobsen, H.L. Skriver, J.K. Nørskov, Phase diagrams for surface alloys, Phys. Rev. B 56 (1997) 5822-5834.

[54] D. Gottschalk, E.A. Hinson, A.S. Baird, H.L. Kitts, K.A. Layman, CO Adsorption on Hydrated Ru/Al_2O_3: Influence of Pretreatment, J. Phys. Chem. C 114 (2010) 4950-4960.

[55] M.F. Brown, R.D. Gonzalez, An Infrared Study of the Adsorption of Carbon Monoxide on the Reduced and Oxidized Forms on Silica- Supported Ruthenium, J. Phys. Chem. 80 (1976) 1731-1735.

[56] M.L. Unland, Isocyanate intermediates in the reaction of NO and CO over noble metal catalysts, J. Catal. 31 (1973) 459-465.

[57] M.H. Kim, J.R. Ebner, R.M. Friedman, M.A. Vannice, Determination of Metal Dispersion and Surface Composition in Supported Cu–Pt Catalysts, J. Catal. 208 (2002) 381–392.

[58] K. Hadjiivanov, H. Knözinger, FTIR Study of Low-Temperature CO Adsorption on Cu-ZSM-5: Evidence of the Formation of $Cu^{2+}(CO)_2$ Species, J. Catal. 191 (2000) 480–485.

[59] T. Miyazawa, S. Koso, K. Kunimori, K. Tomishige, Development of a Ru/C catalyst for glycerol hydrogenolysis in combination with an ion-exchange resin, Appl. Catal. A – Gen. 318 (2007) 244–251.

[60] T. Miyazawa, S. Koso, K. Kunimori, K. Tomishige, Glycerol hydrogenolysis to 1,2-propanediol catalyzed by a heat-resistant ion-exchange resin combined with Ru/C, Appl. Catal. A – Gen. 329 (2007) 30-35.

[61] T. Miyazawa, S. Koso, K. Kunimori, K. Tomishige, Glycerol conversion in the aqueous solution under hydrogen over Ru/C + an ion-exchange resin and its reaction mechanism, J. Catal. 240 (2006) 213–221.

[62] I. Furikado, T. Miyazawa, S. Koso, A. Shimao, K. Kunimori, K. Tomishige, Catalytic performance of Rh/SiO2 in glycerol reaction under hydrogen, Green Chem. 9 (2007) 582–588.

[63] M. Boudart, Turnover rates in heterogeneous catalysis, Chem. Rev. 95 (1995) 661-666.

[64] D.G. Lahr, B.H. Shanks, Effect of sulfur and temperature on ruthenium-catalyzed glycerol hydrogenolysis to glycols, J. Catal. 232 (2005) 386-394.

[65] J.H. Sinfelt, Y.H. Lam, J.A. Cusumano, A.E. Barnett, Nature of ruthenium-copper catalysts, J. Catal. 42(1976)227–237.

[66] E. van Ryneveld, A.S. Mahomed, P.S. van Heerden, H.B. Friedrich, Direct Hydrogenolysis of Highly Concentrated Glycerol Solutions Over Supported Ru, Pd and Pt Catalyst Systems, Catal. Lett. 141 (2011) 958–967.

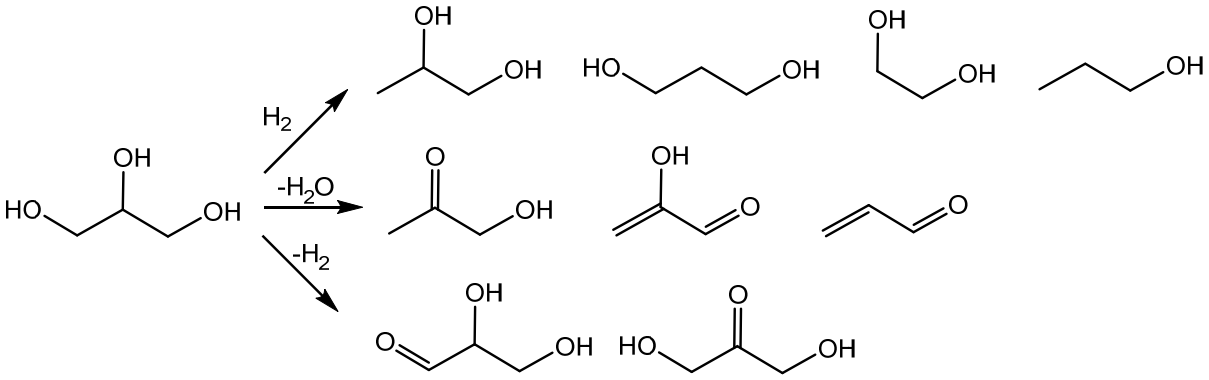

Figure 1: Possible products of glycerol hydrogenolysis, dehydration and dehydrogenation.

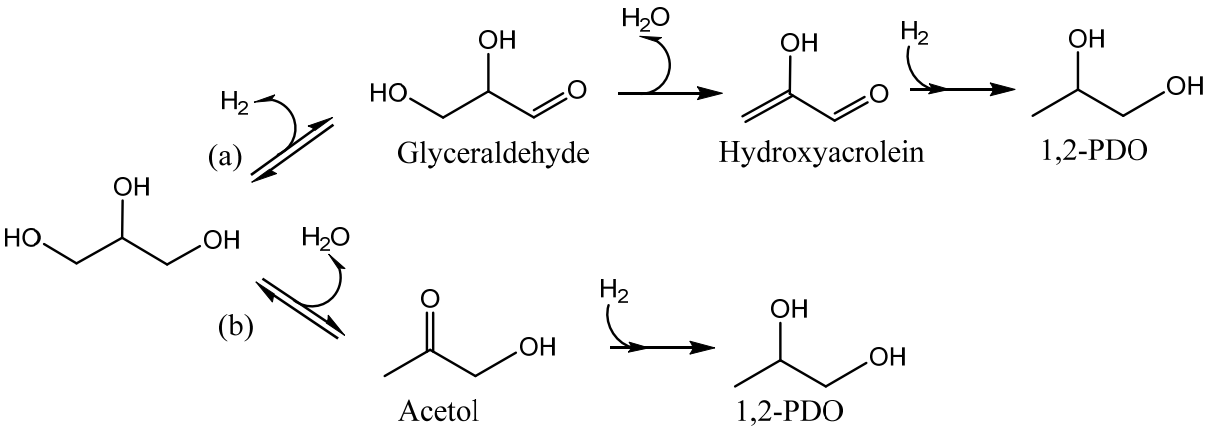

Figure 2: Proposed mechanisms for 1,2-PDO production through glycerol hydrogenolysis.

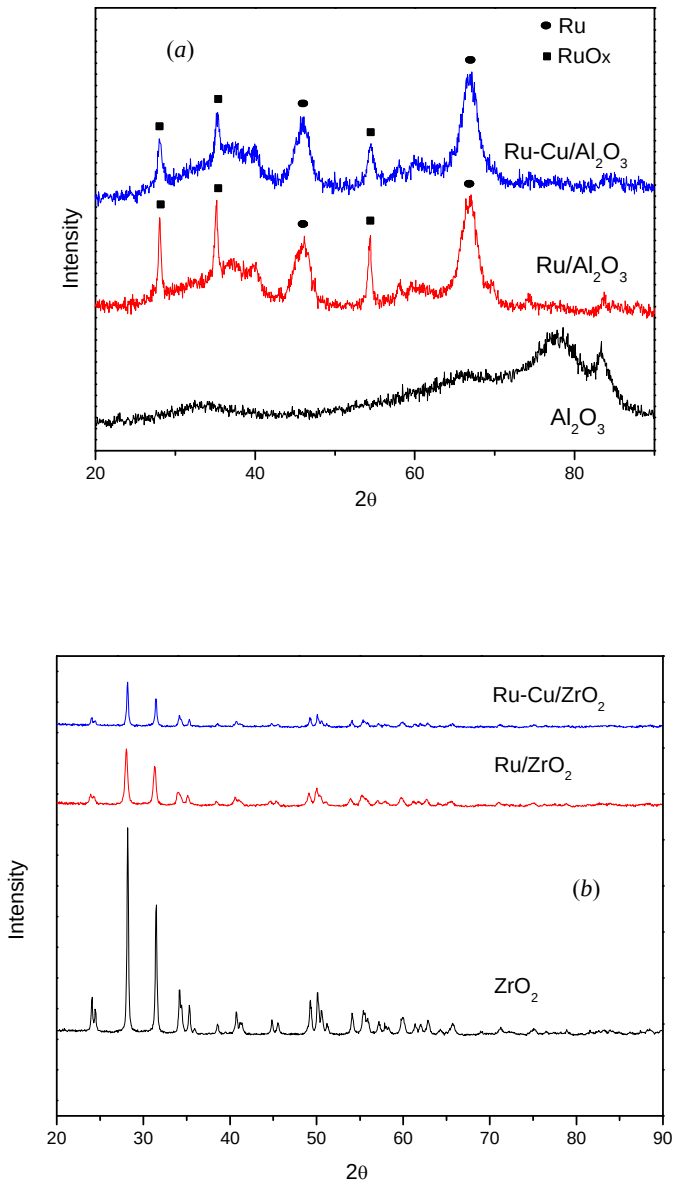

Figure 3: X-ray diffractograms for (a) Al_2O_3, Ru/Al_2O_3, $Ru\text{-}Cu/Al_2O_3$; (b) ZrO_2, Ru/ZrO_2.

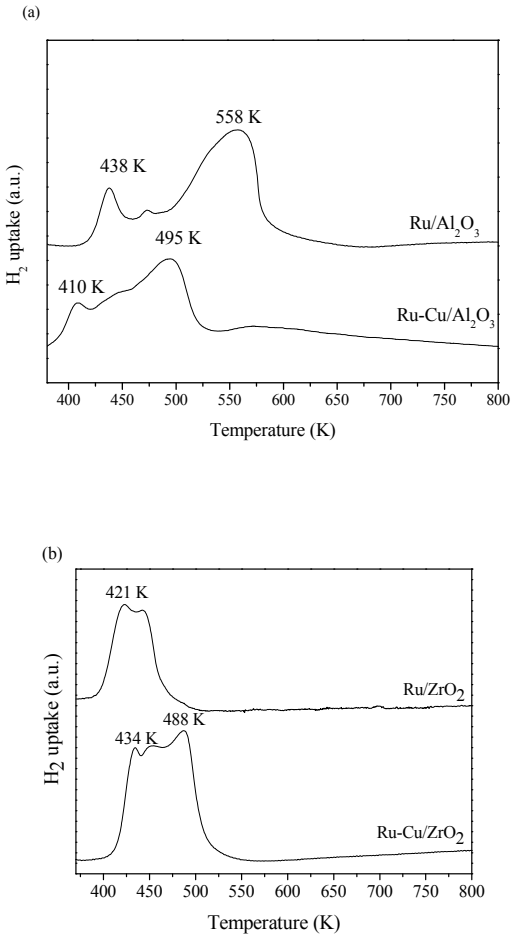

Figure 4: Temperature Programmed Reduction of (a) Ru/Al_2O_3, $Ru\text{-}Cu/Al_2O_3$ and Cu/Al_2O_3; (b) Ru/ZrO_2, $Ru\text{-}CuZrO_2$.

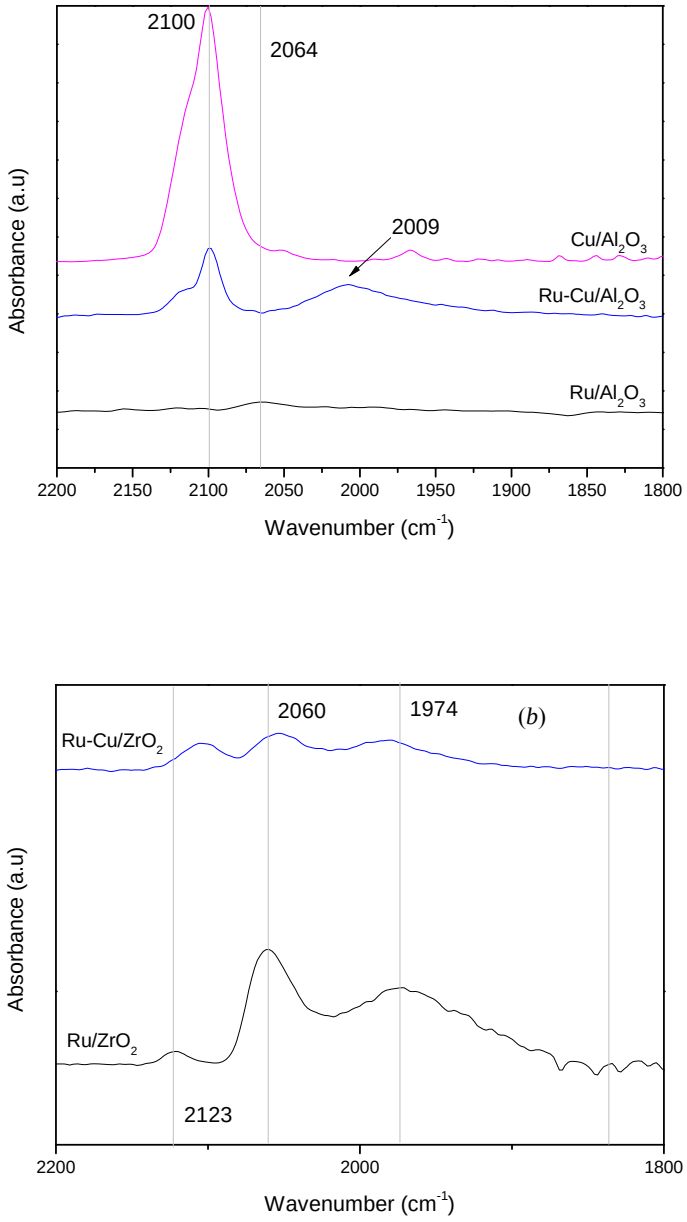

Figure 5: Carbon monoxide DRIFTS at 303 K of (a) Ru/Al_2O_3, Cu/Al_2O_3 and $Ru\text{-}Cu/Al_2O_3$ catalysts; (b) Ru/ZrO_2 and $Ru\text{-}Cu/ZrO_2$ catalysts.

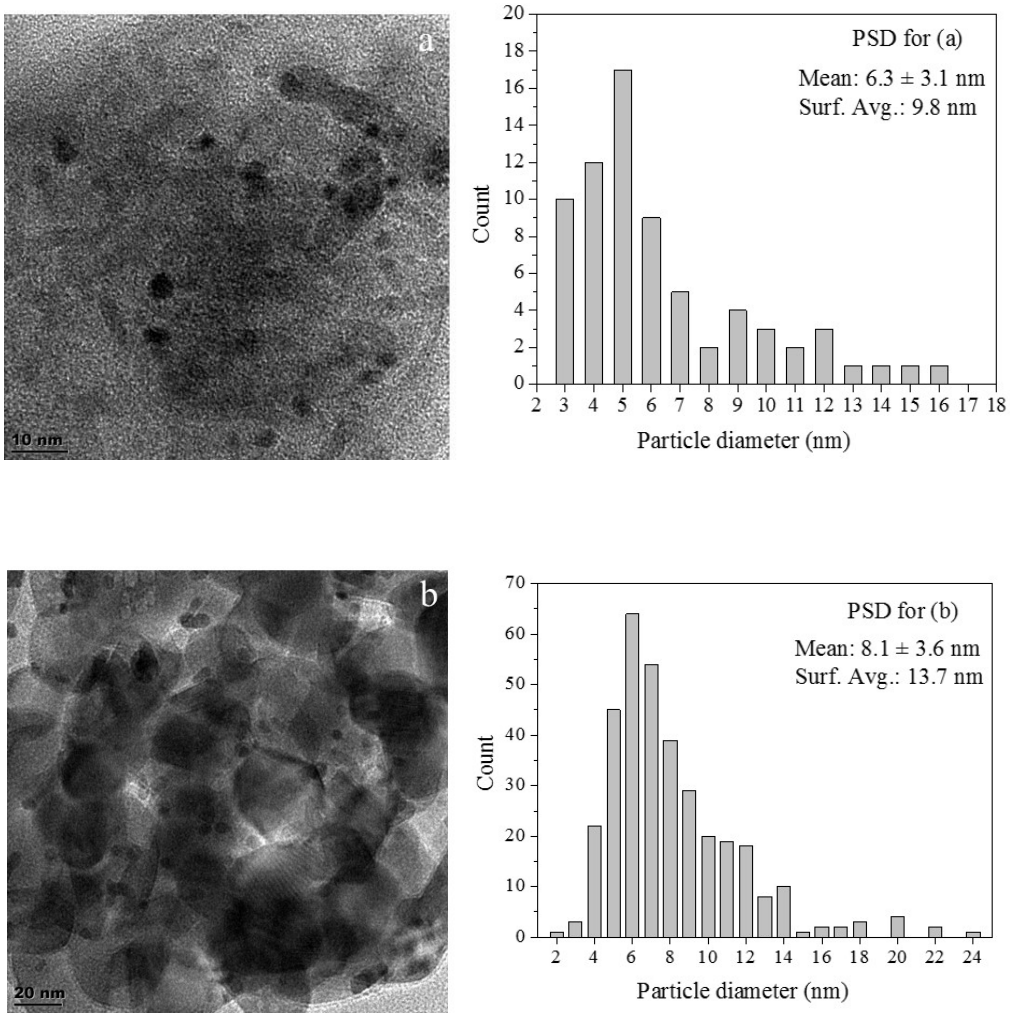

Figure 6: TEM micrographs and the respective diameter size distribution of (a) Ru/Al_2O_3; (b) Ru/ZrO_2.

Table 1. BET surface area, pore volume, metal dispersion results by H chemisorption, and transmission electron microscopy (TEM) particle analysis for Ru supported catalysts.

Catalyst	Surface area (m^2/gcat)	Pore volume (cm^3/gcat)	H_2 $\mu mol/g_{cat}$	Fraction of Ru Exposed (H/Ru)	TEM particle diameter (nm)	Surface average diameter (nm)
Al_2O_3	193	0.80	-	-	-	-
Ru/Al_2O_3	178	0.42	77.0	0.623	6.3 ± 3.1	9.8
$Ru\text{-}Cu/Al_2O_3$	177	0.39	69.2	0.560	10.7 ± 6.1	14.8
ZrO_2	19	0.08	-	-	-	-
Ru/ZrO_2	18	0.08	4.3	0.035	8.1 ± 3.6	13.7
$Ru\text{-}Cu/ZrO_2$	9	0.07	11.9	0.096	10.2 ± 9.1	12.8

Table 2. Results of TPR analysis for Ru based catalysts.

Catalyst	Catalyst mass (mg)	H_2 consumption (mmol)	Reduction efficiency* (%)
Ru/Al_2O_3	503.6	0.337	91.3
$Ru\text{-}Cu/Al_2O_3$	484.0	0.525	97.3
Ru/ZrO_2	509.8	0.314	84.1
$Ru\text{-}Cu/ZrO_2$	422.3	0.482	100.0

*Calculated taking RuO_3 and CuO as the species subject to total reduction.

Table 3. Activity and selectivity for Ru catalysts in glycerol hydrogenolysis.

Catalyst	Conversion (%)[a]	$TOF_0/10^{-3}$ (s^{-1})[b]	Selectivity %			
			1,2-PDO	E.G.	1,3-PDO	Others[c]
Ru/Al_2O_3	32.8	5.1	41.7	42.9	2.1	13.3
$Ru\text{-}Cu/Al_2O_3$	20.6	3.2	91.9	3.7	-	4.4
Ru/ZrO_2	30.1	80.5	69.8	27.6	-	2.6
$Ru\text{-}Cu/ZrO_2$	13.7	11.5	100.0	-	-	-

*Reaction conditions: 20 wt% gly solution; T: 453K; H_2 Pressure: 2.5 MPa; 500 rpm, 24h

[a]Based on total liquid phase products.

[b]Based on total liquid phase products normalized to the H_2 chemisorption capacity of the fresh catalyst

[c]Products considering liquid phase: 1-propanol, 2-propanol, ethanol, methanol, and acetol

Table 4. Comparison of conversion and selectivity for the hydrogenolysis of glycerol on several Ru based catalysts.

Catalysts	Conversion (%)	Selectivity (%)	References
		1,2-PDO	
Ru/Al_2O_3[a]	45.6	59.2	21
Ru/Al_2O_3[b]	69.0	37.9	32
Ru/Al_2O_3[c]	32.8	41.7	This work
Ru/ZrO_2[b]	40.5	60.5	32
Ru/ZrO_2[c]	30.1	69.8	This work
Ru/C[d]	49.2	74	56
$3\%Ru\text{-}0.19\%Cu/Al_2O_3$[e]	68.0	37.0	33
$3\%Ru\text{-}1\%Cu/Al_2O_3$[f]	100	85	29
$3\%Ru\text{-}0.19\%Cu/ZrO_2$[e]	100	84	33
$2.5\%Ru\text{-}2.5\%Cu/Al_2O_3$[c]	45.0	94	This work

[a] Hydrogen pressure 2.5MPa at 453 K; [b] Hydrogen pressure 8MPa at 513 K; [c] Hydrogen pressure 2.5MPa at 473 K; [d] Hydrogen pressure 8MPa at 403 K; [e] 60 %wt. glycerol aqueous solution, 0.5 mL; reaction temperature, 180ºC; Hydrogen pressure, 10.0 MPa; [f] Hydrogen pressure 8MPa at 503 K.

Table 5. Temperature dependence of conversion, apparent specific velocities, reaction rates and turnover frequencies of glycerol hydrogenolysis reaction over Ru-Cu/Al_2O_3 considering first order kinetics.

Temp. (K)	Conv. (%)[a]	$k_{app}/10^{-6}$ (s^{-1})[b]	$R_{V,0}/10^{-6}$ ($mol.L^{-1}.s^{-1}$)[c]	$R_{m,0}/10^{-6}$ ($mol.g_{cat}^{-1}.s^{-1}$)[d]	$TOF_0/10^{-3}$ (s^{-1})[e]	Selectivity (%)			
						1,2-PDO	EG	1,3-PDO	Others[f]
453	20.6	2.41	5.50	0.44	3.2	91.9	3.7	-	4.4
473	45.0	6.96	15.88	1.26	9.1	94.0	6.0	-	-
493	53.6	9.37	21.39	1.70	12.3	76.8	6.2	0.6	15.8

Hydrogen pressure 2.5MPa, 500 rpm, 1.2 g catalyst, 20%wt. glycerol solution.[a] Based on total liquid phase products; [b] k_{app}: apparent first order rate constants; [c] $R_{V,0}$: initial rate of consumption of glycerol per liquid volume; [d] $R_{m,0}$ initial rate of consumption of glycerol per catalyst gram; [e] Based on total liquid phase products normalized to the H_2 chemisorption capacity of the fresh catalyst; [f] others: 1-propanol, 2-propanol, ethanol, methanol, acetol.

Table 6. Recycle experiments with 2.5%Ru/Al_2O_3 and 2.5%Ru/ZrO_2 catalysts for glycerol hydrogenolysis

Cycle	Catalyst	Conversion (%)[a]	Carbon Balance (%)	$TOF/10^{-3}$ (s^{-1})[b]	Selectivity (%)			
					1,2-PDO	EG	1,3-PDO	Others[c]
1	Ru/Al_2O_3	32.8	84	3.6	42	43	2	13
2	Ru/Al_2O_3	30.8	91	3.5	51	37	5	8
3	Ru/Al_2O_3	24.8	94	2.9	49	34	7	10
1	Ru/ZrO_2	30.1	89	60.0	70	28	0	2
2	Ru/ZrO_2	28.7	90	57.7	65	26	2	7

3	Ru/ZrO_2	12.0	100	27.0	59	34	0	7

*Reaction conditions: 20 wt% gly solution; T: 453K; H_2 Pressure: 2.5 MPa; 500 rpm, 24h. The spent catalyst was recovered by filtration with a 0.45μm pore membrane, washed with distilled, deionized water and dried at 393 K before recycle. [a]Based on total liquid phase products. [b]Based on total liquid phase products normalized to the H_2 chemisorption capacity of the fresh catalyst. [c]Others: 1-propanol, 2-propanol, ethanol, methanol, and acetol